Transmission line unavailability due to correlated threat exposure

Erlend Sandø Kiel
Department of Electric Power Engineering
NTNU - Norwegian University of Science and Technology
Trondheim, Norway
erlend.kiel@ntnu.no

Gerd Hovin Kjølle
Department of Electric Power Engineering
SINTEF Energy Research/NTNU
Trondheim, Norway

***Abstract*—Blackouts in the power system are rare events that can have large consequences for society. Successful preparation and prevention of such events calls for models capable of predicting their occurrence. The simultaneous outage of multiple components is of special interest in an N-1 secure transmission grid. Spatio-temporal correlation in probability of failure for components can cause blackouts to occur more often than anticipated. This paper demonstrates a new method of calculating time-series of component unavailability due to external threats based on historical data. The time-series of unavailability can be used to predict the expected occurrence of contingencies throughout the year. A test case is presented where an hourly time series of wind dependent failure probabilities and historical outage durations of transmission lines are combined to illustrate the proposed method. The results show that the simultaneous unavailability of multiple transmission lines may be significantly larger than estimated using traditional reliability analysis.**

***Index Terms*—Power system reliability, resilience, risk analysis.**

I. Introduction

The electrical power system is a highly complex, critical infrastructure on which society depends. Blackouts are rare but with potentially severe consequences, and due to these properties they are sometimes referred to as High Impact Low Probability (HILP) events. In an N-1 secure transmission grid multiple contingencies, or failure of multiple components, must occur in overlapping time-frames to cause blackouts. Harsh weather, such as wind, lightning and icing are some of the most common causes of transmission line failures and subsequent blackouts [1], [2]. Such events often occur in short and intense periods of weather exposure such as severe storms [3]. The overlap in time and place of failures due to correlated threats is of high importance. The timing of when a contingency occurs can also affect the associated consequences. Thus, it is necessary to develop models that capture spatio-temporal correlation in threat exposure.

Capturing HILP events using traditional power system reliability methods can be difficult. The emerging field of power systems resilience methodology goes beyond traditional reliability assessments and aim to capture such low probability events [3]. Although there are no commonly accepted definition of resilience in the power systems domain, a proposed definition is found in [4] as "the ability to withstand and reduce the magnitude and/or duration of disruptive events, which includes the capability to anticipate, absorb, adapt to, and/or rapidly recover from such an event". In [5], it is argued that "a main difference between a reliable power grid and a resilient power grid is that, in the latter, low probability-high consequence events (e.g. extreme weather events) are specifically considered and handled, with the ability to learn from past occurrences".

The two main paths to capture spatio-temporal correlaction in threat exposure has either been to use Monte Carlo simulation techniques or contingency enumeration approaches, considering multiple weather states [6], [7]. It has been considered that for single contingency events, contingency enumeration may be best suited, however for more complex systems and higher order contingencies Monte Carlo simulation techniques may produce better results [8]–[10].

This paper proposes a method of calculating time-series of unavailability probability of transmission lines based on historical data, and can serve as an alternative to Sequential Monte Carlo simulations. The probability of higher order contingencies can be calculated from the time-series unavailability of single components. The method answers two of the set of risk-triplets put forwards by Kaplan [11], namely what can happen (the scenario) and how likely is it that this scenario happens (likelihood). However, by also knowing the 'when' of the scenario, it is possible to make some inferences of the last of the triplets: the consequence of the scenario.

The main contribution of this article is to calculate time-series of probability of contingencies occurring due to threats that are spatio-temporally correlated. It is also a benefit that each primary parameter in the analysis - the failure rate and outage duration - can be analyzed separately before being combined into an expected unavailability of components. The production of historical time series of unavailability makes it possible to couple the analysis with other time-dependent information, for example measures of consequence of a given contingency in a specific period of time. The method is transparent and the resulting data can form the basis for

The research leading to these results has received funding through the project "Analysis of extraordinary events in power systems" (HILP) (Grant No. 255226), co-funded by the Research Council of Norway, Statnett and Fingrid.

further analysis, or serve as a benchmark when developing other methods for predicting HILP events. The method is exemplified for transmission lines using wind dependent failure- and outage durations, as they are well known to contribute to failure bunching effects in the power system [10], [12]. Results from the analysis can be used, for example, to prioritize maintenance and repair, strengthening of system components, rerouting or undergrounding transmission lines, or improvement of emergency and preparedness plans [10].

The rest of the paper is structured as follows: Section II defines central terms and introduces the practical implementation of the method such as the inclusion of failure rates, outage duration curves and the calculation of unavailability of transmission lines. In Section III, a sample case study on a 4-bus test system is presented to show the relevance of the method, before the paper is concluded in Section IV.

II. Method

The proposed method calculates the expected instantaneous unavailability of transmission lines. The method is exemplified using unplanned transmission line outages due to wind, although the approach can be applied to other components that are subject to spatio-temporally correlated threats. Instantaneous unavailability can be defined as the "probability that an item is not in a state to perform as required at a given instant" [13], where "a given instant" is here understood as the time-scale granularity of the analysis, which is set to one hour in this example. Instantaneous unavailability will from now on simply be referred to as unavailability.

The method consists of three different steps. Initially, a time series of failure probabilities of transmission lines due to wind exposure is either created or served as an input into the analysis. Probability distributions of outage durations are then parameterized using historical data. These outage distributions are then combined with failure probabilities to create a measure of unavailability of transmission lines.

A. Failure probabilities

Time series of hourly failure probabilities can be calculated in a number of ways, depending on data availability and need for accuracy. For weather related phenomena, the combined use of historical failure data and weather conditions as seen in [14], [15] can be of great help to capture historical susceptibility to given threats, as well as failure bunching effects.

Time-series of hourly wind dependent failure probabilities are generated according to the method of [14], with Bayesian updating of failure rates and fragility curve estimation based on historical failure and wind exposure. Initially, unique annual failure rates for each line is calculated by doing a Bayesian updating using the historical average failure rate due to wind of all comparable lines in the system, and actual failures due to wind for individual lines in a given time-span. A fragility curve is then fitted to a wind exposure measure for each line segment to distribute the failures in time, before the probability of failure for each line is calculated as a series system of failure probability of its line segments. The calculated annual failure rate after curve fitting is held equal to the annual failure rate found by Bayesian updating in the previous step to maintain consistency. The weather data used to calculate wind exposure of line segments is historical hourly wind speeds in a 1 kilometer grid based on [16]. A more detailed description of how to construct the time-series of failure probabilities can be found in [14].

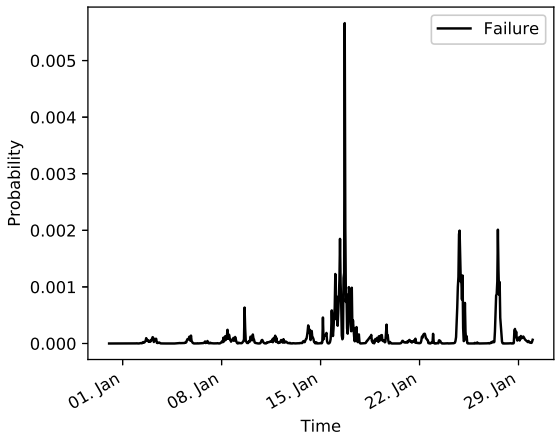

Fig. 1. Hourly probability of line failure. Sample.

In this paper a slight alteration of the original method is done. The fragility curve is not cut off at a lower wind-speed limit. The relatively low probability of failure at the low end of the fragility curve matches well with the historical percentage of failures occurring below 15 m/s wind-speeds at about 20 percent [17], which is the justification of this alteration. A sample of the calculated hourly failure probabilities due to wind exposure for one line can be seen in Fig. 1, showing the hourly probability of failure for a transmission line due to wind exposure.

B. Outage duration

Events caused by natural hazards are also associated with longer outage durations due to mechanical damage or limitation to accessibility for repairs [1], [18]. The aim of the following subsection is to create an outage duration curve that represents the probability of a component still being out of operation a given number of hours following a failure caused by wind exposure.

Outage duration curves is constructed using data from the Norwegian fault and disturbance database, FASIT [17], [19]. The database contains information on historical failures of components, delivery point interruptions, and restoration and repair times. Outage duration is here understood as the time from a failure occurs until the component is again ready for operation and covers both temporary and permanent failures.

The outage durations due to wind exposure from the FASIT data show a right skewed distribution of outage durations as shown in the histogram in Fig. 2. Other sources of outage and repair statistics show similar patterns [20], [21]. The two-parameter log-normal distribution is a good choice to represent

the data, which is in line with what was found by [20]. The log-normal distribution is given by (1), where $f(r)$ is the probability density function (PDF) of the distribution of outage durations of r hours.

$$f(r) = \frac{1}{r\sigma\sqrt{2\pi}} e^{-\frac{(ln(r)-\mu)^2}{2\sigma^2}} \tag{1}$$

The moments found from the FASIT data are then used to fit a log-normal PDF of outage duration by modifying the equations for the mean and variance. The method of moments approach is used to ensure that the mean and variance found in the data is maintained. The mean (2) and variance (3) of the outage duration data is used to fit the parameters of the log-normal distribution in (4) and (5). D represents the random variable of outage duration, while d_i represents the unique outage duration observations in hours.

$$E(D) = \frac{1}{n}\sum_{i=1}^{n} d_i \tag{2}$$

$$Var(D) = \frac{\sum_{i=1}^{n}(d_i - E(D))^2}{n-1} \tag{3}$$

$$\mu = ln\left[\frac{E(D)^2}{\sqrt{Var(D)+E(D)^2}}\right] \tag{4}$$

$$\sigma = \sqrt{ln\left[1+\frac{Var(D)}{E(D)^2}\right]} \tag{5}$$

Furthermore, we want to know the probability that a component has not been restored by a given time, x. This can be found through the survival function (SF) of the distribution. The survival function $S(x)$ is the complement of the cumulative distribution function (CDF) denoted $F(x)$, and can be expressed as in (6).

$$S(x) = 1 - F(x) = 1 - \int_0^x f(r)dr \tag{6}$$

The function now describes the probability that a component is in a failed state for a given number of hours after a failure event. The original outage duration data and the fitted distribution can be seen in Fig. 2. However, the outage duration function is a continuous distribution while the time-series is in one-hour intervals. To account for this, the approximate mean value of each time-step is calculated using the trapezoidal rule.

C. Unavailability probability

When failure probabilities are combined with outage duration probabilities, we get a measure of probability of the line being unavailable at a given time. Unavailability is calculated algorithmically by looping through failure probability time-series and applying the outage probability functions. The logic behind the approach is best illustrated in pseudo-code, seen in Algorithm 1. After looping through all time-steps, an approximation of the expected unavailability of the transmission line at a given time is achieved. The algorithm shows only the calculation of unavailability for a single transmission line but can be repeatedly applied to any number of components.

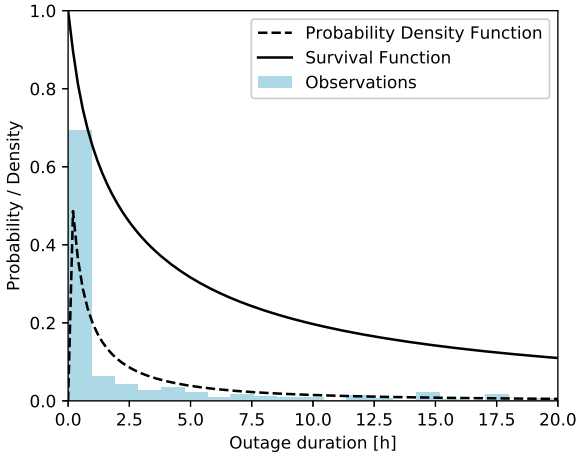

Fig. 2. Observed outage duration of power lines (132-420kV) 2006-2016.

The algorithm appends the expected unavailability at time *t* to a given number of time-steps *x* ahead of time up until a given cutoff, taking into account the probability that the line is already unavailable due to a previous failure. The cutoff in forward looking time-steps is a trade-off between computational efficiency and accuracy, and is set to 1000 hours after the failure in this example.

To correct for the accuracy impact of the chosen 1000 hour cutoff, we need to compare the area under the SF-curve when considering the integration of the curve towards infinity versus an upper bound of 1000 hours. For the former, the alternative expectation formula (see e.g. [22]) is used, which states that the integral from zero to infinity of the SF for a continuous non-negative random variable equals the expected value of the distribution (7). For the latter, numerical integration is used to approximate the area under the curve. The ratio of these two areas, k in (8), can then be used to inflate numbers before the cutoff. This ensures that the sum of outage duration is kept the same as without a cutoff.

$$E(X) = \int_0^\infty [1 - F(x)]dx \tag{7}$$

$$\frac{E(D)}{\int_0^{1000}[1-F(x)]dx} = k \tag{8}$$

The result of running the algorithm is given in Fig. 3, which shows the hourly expected unavailability due to wind for a single transmission line using the proposed method. The figure is based on the failure probabilities found in Fig. 1 and outage duration curve in Fig. 2.

Algorithm 1 Algorithm for calculating unavailability

Input: time-series of t failure probabilities
Output: time-series of t unavailability probabilities

Initialisation:
$p_t \leftarrow$ failure probability at time t
$S(x) \leftarrow$ outage survival function at time x since failure
$u_t \leftarrow$ unavailability probability at time t
cutoff $\leftarrow$ limit to forward propagating time-steps
$k \leftarrow$ inflation factor due to cutoff
LOOP Process:

1: **for** all increasing time steps t **do**
2: **for** x in $range(0, cutoff)$ **do**
3: $u_{t+x} += p_t \cdot (1 - u_t) \cdot S(x) \cdot k$
4: **end for**
5: **end for**
6: **return** u_t

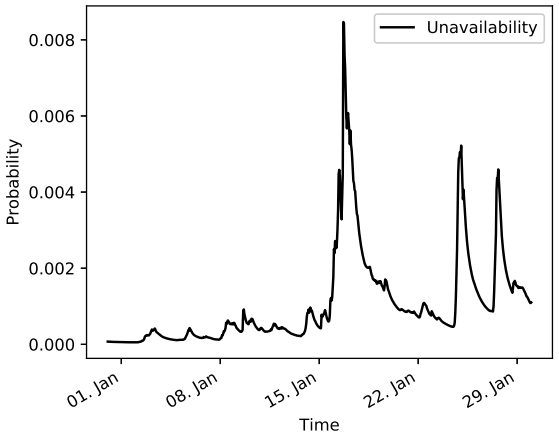

Fig. 3. Hourly probability of line unavailability. Sample.

III. Sample case

The goal of this approach is to better capture spatio-temporal correlations in unavailability due to weather. A test case is presented to exemplify. Unavailability is calculated using both the proposed method, and a traditional analytical method paired with a contingency enumeration approach [23] as the base case. The results are then compared.

A 4-bus test network, given in [24], presented in [25], is used to illustrate the test case. The 4-bus test network can be seen in Fig. 4. Every line in the test-network is given a capacity of 135 MW. Both generators have the capacity to cover all demand on their own. Load point 1 (L1) is the prioritized load point due to a higher cost of Energy Not Supplied (ENS). Only minimal cutsets are enumerated. Two operating states (OS) are considered, a high- and a light-load state, which have their own minimal cuts. The high demand state (OS2) covers the months December, January and February, while the light-load state (OS1) covers the remaining months.

A divergence from the original test case is that individual reliability input data for overhead transmission lines in the test network is calculated, based on historical weather and outage durations. This is done to ensure that the same mean values are used in both the base case and the proposed method. The modified rating and reliability data is given in Table I. The delivery point load demand for the different operating states are given in Table II. Minimal cut-sets (MC) are associated with an interrupted power (P_{interr}) at specific delivery points (DP) in different operating states (OS), given in Table III.

The base case is a contingency enumeration approach using average failure rates and outage durations as input to the evaluation of the unavailability of the components. Approximate methods are used to calculate equivalent failure rates, outage durations and unavailability for higher order contingencies. Equations for this can be found in any number of reliability textbooks, see e.g. [26]. Expected annual unavailability for each operating state and delivery point is calculated as the product of the annual failure rate and outage duration weighted according to the duration of each operating state, exemplified

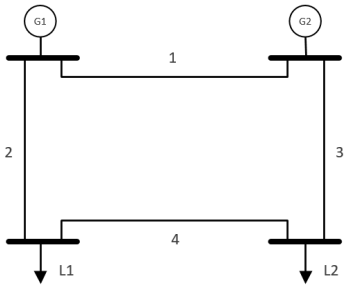

Fig. 4. 4-bus OPAL network [24].

TABLE I
Modified rating and reliability data, transmission lines

Line	Rating [MW]	Failure rate [failures/year]	Outage time [hours/failure]
1	135	0.118	11.42
2	135	0.375	11.42
3	135	0.069	11.42
4	135	0.229	11.42

TABLE II
Delivery point load demand

DP	Light load (OS1) [MW]	Heavy load (OS2) [MW]
L1	60	100
L2	30	75

TABLE III
Interrupted power [MW] due to minimal cutsets (MC)

	Light load (OS1)		Heavy load (OS2)	
MC\DP	L1	L2	L1	L2
{2}	-	-	-	40
{3}	-	-	-	40
{2,3}	60	30	100	-
{2,4}	60	-	100	-
{3,4}	-	30	-	-

in (9) for OS1 (9 out of 12 months). Expected Annual ENS (AENS) is calculated as in (10).

$$U_{MC,OS1} = \lambda_{MC} \cdot r_{MC} \cdot \frac{9}{12} \tag{9}$$

$$AENS_{MC,OS,DP} = U_{MC,OS} \cdot P_{interr,MC,OS,DP} \tag{10}$$

The proposed method relies on the same minimal cutsets and power interrupted, and has the same average failure rates and outage times as the base case. However, the input to the reliability evaluation is time series of failure probabilities and distributions of outage durations. Time series of hourly unavailability covering 25 years of observations for four transmission lines is constructed using historical weather data and outage durations. Single line contingencies are calculated using the proposed algorithm. The correlation of failure probabilities between lines are given in Table IV. Higher order contingencies can be calculated as a system of independent components in parallel (see e.g. [27]) given the weather exposure. The expected unavailability of the resulting time series, u_t, in the months of the different operating states can be summed up and adjusted for the number of years of observations, y, to find annual unavailability of the cutsets in the associated operating states, as seen in (11).

$$U_{OS} = \frac{\sum_{t=1,t\in OS}^{n} u_t}{y} \tag{11}$$

TABLE IV
CORRELATION OF FAILURE PROBABILITIES BETWEEN LINES

		Line			
		1	*2*	*3*	*4*
Line	*1*	1.00	0.74	0.17	0.60
	2	0.74	1.00	0.11	0.57
	3	0.17	0.11	1.00	0.21
	4	0.60	0.57	0.21	1.00

The calculated expected annual unavailability and AENS are compared in the different approaches. Single line unavailability can be seen in Fig. 5. Numbers in bars represent the percentage difference in unavailability when comparing the proposed method to the base case for each operating state. Although single line contingencies occur with the same expected number of hours each year in the two approaches, the displacement of when unavailability occurs has an effect on ENS, as single line contingencies only cause ENS in OS2. The difference in ENS as a result of this displacement can be observed in Table V. ENS during OS2 for line 2 and 3 is 82% and 79% higher respectively, using the proposed method than in the base case. This is a reflection of harsher weather during the winter months which is more accurately captured by the time-series unavailability in the proposed method.

Spatio-temporal correlations and the associated failure bunching come into play for second order contingencies. The total unavailability of second order contingencies have notably lower estimates during the winter months in the base case compared to the proposed method, especially when failure

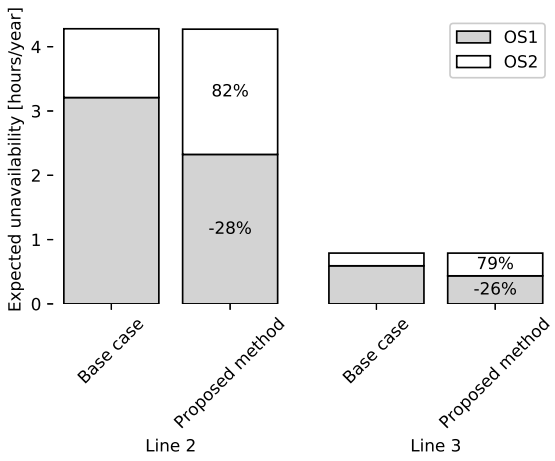

Fig. 5. Single line unavailability in different operating states.

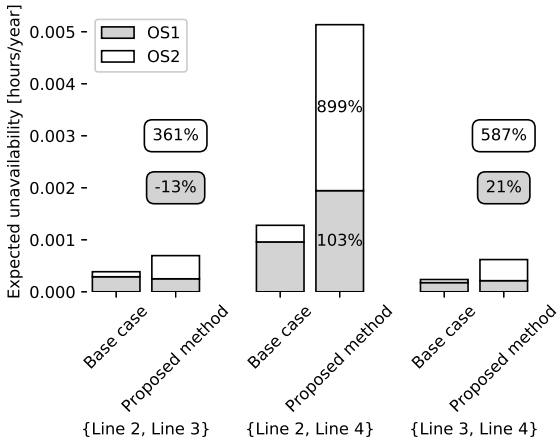

Fig. 6. Unavailability due to second order contingencies

probabilities are highly correlated. Results in Fig. 6 illustrate this: Unavailability of the minimal cutset lines 2 and 4 due to wind in OS2 is 899% higher than in the base case, and the annual ENS is 387% higher. The reason for this increase is two-fold. First, the hourly average expected unavailability is higher during the winter months in this sample. Secondly, periods of high expected unavailability for the two components coincide due to spatio-temporal correlation in weather exposure for this cutset, thus causing the product of the two probabilities to sum to larger values than if this was not the case. This effect is not captured by the base case method.

Single line contingencies dominate the expected annual unavailability and ENS, compared to the second order contingencies. However, the effects of higher order contingencies are more relevant to consider in a N-1 secure transmission grid. The difference in expected annual unavailability and ENS is 239% and 290% higher, respectively, compared with the base case for second order contingencies.

TABLE V
SUMMARY RESULTS

	Base case	Proposed method	Δ
Unavailability [h/y]			
Line 2	4.2789	4.2726	0 %
Line 3	0.7901	0.7897	0 %
Line 2 Line 3	0.0004	0.0007	80 %
Line 2 Line 4	0.0013	0.0051	302 %
Line 3 Line 4	0.0002	0.0006	163 %
Single lines	5.0689	5.0623	0 %
2nd order contingencies	0.0019	0.0065	239 %
Total	5.0708	5.0687	0 %
AENS [MWh/y]			
Line 2	42.7886	77.9177	82 %
Line 3	7.9005	14.1269	79 %
Line 2 Line 3	0.0357	0.0670	88 %
Line 2 Line 4	0.0895	0.4358	387 %
Line 3 Line 4	0.0053	0.0064	21 %
Single lines	50.6891	92.0445	82 %
2nd order contingencies	0.1305	0.5093	290 %
Total	50.8195	92.5538	82 %

IV. CONCLUSION

In this paper we have developed a method of calculating time-series unavailability of components in the electrical transmission system due to external threats that exhibit spatio-temporal correlation. The solution is exemplified in a test case, which shows that the proposed method captures spatio-temporal correlation in threat exposure more accurately than the base case method. When combining the time-series output of expected unavailability with a consequence analyses we get a more complete view of the associated risks. In the test case, this results in an almost four times higher AENS due to a second order cutset with highly correlated wind exposure.

The proposed method must make a trade-off between the need for accuracy and computational efficiency, and as a consequence it relies on several approximations in distributing outage durations in time. However, comparison of single line contingencies show that there are small differences in annual expected unavailability in the approaches, which indicates that the effects of the approximations are limited. It can be argued that the benefits of capturing the spatio-temporal correlations in the analysis of higher order contingencies outweighs the negative impact of these approximations.

By identifying lines that has a high impact on a given consequence metric, such as ENS, in conjunction with other lines, strengthening measures can be prioritized and initiated on lines that have the greatest consequence reducing effects. The proposed method is a useful approach that may contribute to reducing the probability of HILP events and thereby, to a more resilient grid.

REFERENCES

[1] Y. Wang, C. Chen, J. Wang, and R. Baldick, "Research on Resilience of Power Systems Under Natural Disasters—A Review," *IEEE Transactions on Power Systems*, vol. 31, no. 2, pp. 1604–1613, Mar. 2016.

[2] E. Bompard, T. Huang, Y. Wu, and M. Cremenescu, "Classification and trend analysis of threats origins to the security of power systems," *International Journal of Electrical Power & Energy Systems*, vol. 50, pp. 50–64, Sep. 2013.

[3] M. Panteli, P. Mancarella, D. Trakas, E. Kyriakides, and N. Hatziargyriou, "Metrics and quantification of operational and infrastructure resilience in power systems," *IEEE Transactions on Power Systems*, vol. 32, no. 6, pp. 4732–4742, 2017.

[4] A. Stankovic, "The Definition and Quantification of Resilience," IEEE PES Industry Tech. Support Task Force, Tech. Rep. PES-TR65, 2018.

[5] R. Rocchetta, E. Zio, and E. Patelli, "A power-flow emulator approach for resilience assessment of repairable power grids subject to weather-induced failures and data deficiency," *Applied Energy*, vol. 210, pp. 339–350, Jan. 2018.

[6] GARPUR, "D1.1 State of the art on reliability assessment in power systems," SINTEF Energi AS, Tech. Rep. 608540, Mar. 2014.

[7] R. Billinton, C. Wu, and G. Singh, "Extreme adverse weather modeling in transmission and distribution system reliability evaluation," in *PSCC*, Sevilla, 2002.

[8] A. M. Rei, M. T. Schilling, and A. C. G. Melo, "Monte Carlo Simulation and Contingency Enumeration in Bulk Power Systems Reliability Assessment," in *PMAPS*, Stockholm, 2006.

[9] M. Panteli and P. Mancarella, "Influence of extreme weather and climate change on the resilience of power systems: Impacts and possible mitigation strategies," *Electric Power Systems Research*, vol. 127, pp. 259–270, Oct. 2015.

[10] M. Panteli and P. Mancarella, "Modeling and Evaluating the Resilience of Critical Electrical Power Infrastructure to Extreme Weather Events," *IEEE Systems Journal*, vol. PP, no. 99, pp. 1–10, 2015.

[11] S. Kaplan and B. J. Garrick, "On The Quantitative Definition of Risk," *Risk Analysis*, vol. 1, no. 1, pp. 11–27, Mar. 1981.

[12] R. Billinton, G. Singh, and J. Acharya, "Failure Bunching Phenomena in Electric Power Transmission Systems," *Proceedings of the Institution of Mechanical Engineers, Part O: Journal of Risk and Reliability*, vol. 220, no. 1, pp. 1–7, Jan. 2006.

[13] International Electrotechnical Commission, "International Electrotechnical Vocabulary. IEV number 192-08-04."

[14] Ø. R. Solheim, G. Kjølle, and T. Trötscher, "Wind dependent failure rates for overhead transmission lines using reanalysis data and a Bayesian updating scheme," in *PMAPS*, Beijing, 2016.

[15] Ø. R. Solheim and T. Trötscher, "Modelling transmission line failures due to lightning using reanalysis data and a Bayesian updating scheme," in *PMAPS*, Boise, 2018.

[16] Kjeller Vindteknikk, "Long-term data series, WRF ERA-Interim." [Online]. Available: http://www.vindteknikk.com/services/analyses/wind-power/pre-construction/long-term-series-2

[17] G. Kjølle, A. O. Eggen, H. M. Vefsnmo, J. Heggset, A. Bostad, T. Trötscher, and Ø. R. Solheim, "Norwegian disturbance management system and database," in *CIGRE, Session Proceedings 2016*, Paris, 2016.

[18] E. Hillberg, "Perception, Prediction and Prevention of Extraordinary Events in the Power System," Doctoral Theses, Norwegian University of Science and Technology, Trondheim, Norway, Jan. 2016.

[19] J. Heggset, G. Kjolle, and K. Sagen, "FASIT - a tool for collection, calculation and reporting of reliability data," in *IET Conference Publications*. Prague, Czech Republic: IET, 2009, pp. 716–716.

[20] A. Arif and Z. Wang, "Distribution Network Outage Data Analysis and Repair Time Prediction Using Deep Learning," in *PMAPS*, Boise, 2018.

[21] B. Shen, D. Koval, and S. Shen, "Modelling extreme-weather-related transmission line outages," in *1999 IEEE Canadian Conference on Electrical and Computer Engineering*, vol. 3. Edmonton, Alta., Canada: IEEE, 1999, pp. 1271–1276.

[22] S. Chakraborti, F. Jardim, and E. Epprecht, "Higher-Order Moments Using the Survival Function: The Alternative Expectation Formula," *The American Statistician*, pp. 1–4, Jul. 2017.

[23] O. Gjerde, G. Kjølle, S. H. Jakobsen, and V. V. Vadlamudi, "Enhanced method for reliability of supply assessment - an integrated approach," in *PSCC*. IEEE, 2016.

[24] G. Kjølle and O. Gjerde, "The OPAL methodology for reliability analysis of power systems," SINTEF Energy Research, Technical Report TR A7175, Jul. 2012.

[25] G. H. Kjølle, I. B. Sperstad, and S. H. Jakobsen, "Interruption costs and time dependencies in quality of supply regulation," in *PMAPS*, Durham, 2014.

[26] R. Billinton and R. N. Allan, *Reliability Evaluation of Power Systems*, 2nd ed. New York, NY, USA: Plenum Press, 1996.

[27] M. Rausand and A. Høyland, *System reliability theory: models, statistical methods, and applications*, 2nd ed., ser. Wiley series in probability and statistics. Hoboken, NJ: Wiley-Interscience, 2004.